Unsteady simulation of the painting process with high speed rotary bells

J. Domnick[1], A. Scheibe, Q. Ye*
University of Applied Sciences Esslingen
Kanalstrasse 33, 73728 Esslingen, Germany
*Institut für Industrielle Fertigung und Fabrikbetrieb,
University of Stuttgart, Nobelstrasse 12, 70569 Stuttgart, Germany

Abstract

High-speed rotary bells are widely used in automotive industry, as they provide high quality paint films. To obtain reasonably high transfer efficiencies, the paint droplets are charged immediately at the atomizer, leading to an additional electrical force on the droplets directing them towards the grounded target.

As an extension of previous work of the authors related to the simulation of electrostatically supported painting, this paper describes new results of the true dynamic painting process with moving atomizers. As before, the commercial program FLUENT has been used as a vehicle, with complementary subroutines to account for the unsteady charging of the droplets, the calculation of the static electric field and the space charge effect. The dynamic meshing approach has been chosen to calculate the unsteady grid between moving atomizer and fixed target. The calculation domain has basically been divided into a static zone (fixed target), a moving zone (moving atomizer) and a dynamic zone outside the major spray cone.

Concerning the main purpose of these calculations, i. e. the local thickness of the paint film on the target, the dynamic calculations presented herein deliver a very good agreement with experimental results. Local differences even on complex targets are typically less than 2 µm, which is within the reproducibility of the experiments.

In general, this approach can be used to simulate the painting process of almost arbitrary geometries. The dynamic mesh model presented is, together with all the extensions described above, compatible with the current FLUENT code and can be fully parallelized. Nevertheless, there are still several steps to go before this approach can be used directly to solve industrial problems. On a state of the art PC-type computer, CPU time is several days to calculate 1,5 m of atomizer movement.

Introduction

In the last few years, the numerical simulation of the spray painting process for the automotive industry has obtained increasing interest. The estimation of the local paint film thickness during the painting process is one of the key issues for a future realization of the virtual paint shop as part of the so-called digital factory. The final aim of this approach is to simulate the complete production process, including also the estimation of important features of the final product. With respect to the painting process, spray coating is one of the core processes that need to be modeled and simulated. In state-of-the-art automotive paint shops, mainly high speed rotary atomizers are applied. Through an additional electrostatic support, this kind of atomizer combines a high quality paint film with reasonable transfer efficiencies, i.e. fraction of the atomized paint mass that finally deposits on the target.

Especially in the last 5 years, the simulation of the electrostatically supported spray painting process has been treated in a number of scientific contributions. Commercial CFD-codes like FLUENT have been extended to account for the specific features of the flow field and the propagation of the paint droplets, including

- The calculation of the static electrical field between the atomizer and the grounded substrate
- The different charging mechanisms, i.e. direct charging through contact of the paint with charged surfaces and corona charging through the interaction of the paint droplets with free ions
- The effect of space charge due to the charged droplets as well as the free ions in the case of corona discharging.
- The ion wind as a result of the ion flux density.

Basically, the Euler-Lagriagian approach has been used to calculate the flow field and the droplet trajectories, extended by the additional electrical forces that act on the individual droplet. Finally, the final paint film thickness is calculated from the local mass flux of the droplet that reaches a certain area on the target. Similarly, the transfer efficiency is obtained.

[1] Corresponding author

Unfortunately, the painting process is inherently unsteady, as the atomizer is moving permanently across the target to achieve a more or less homogeneous film thickness on the whole substrate surface. As a result, the instantaneous geometry that has to be simulated is changing constantly. Very basic features of the process such as the form the of electric field change in time and require an unsteady simulation approach. Of course, this leads to a significant increase in the necessary computer power and capacity and, hence, in computational time. Therefore, the unsteady character of the flow has been taken into account through a more pragmatic approach, so far. From the simulation of the so-called static film thickness distribution, i.e. a calculation with fixed atomizer, the local static film thicknesses could be obtained on the surface of arbitrary 3D-objects. This static film thickness has been used to derive the dynamic film thickness by artificially moving the spray pattern along a given path on the substrate and integrating the mass in the direction of propagation. Of course, reasonable results can only be obtained as long as the geometry of the substrate in the direction of atomizer movement does not vary significantly. Therefore, several static spray patterns had to be calculated to be able to paint a more complex target.

As an extension of the previous work described above, the present paper deals with true unsteady simulations of the electrostatically supported spray painting process with high speed rotary bells involving unsteady flow calculations and dynamic meshing models. Again, the simulations are based on the commercial FLUENT code, offering appropriate dynamic meshing models. The simulated film thickness distributions are compared with the experimental results.

Experimental Set-up and Atomizer Characteristics

The investigations shown here were made with an external charging state-of-the-art high-speed rotary bell atomizer (Dürr Systems GmbH) used in automated paint applications. Front view and cross section of the atomizer are depicted in Fig. 1. After disintegration at the bell edge, the droplets propagating mainly radially outward are exposed to the axially directed shaping air, redirecting them to the region in front of 6 or 8 electrodes. At these electrodes, corona discharges are produced due to the high potential at the corona needles, finally charging the droplets through the interaction with the ions formed. Both shaping air and electrical form acting on the charged droplets direct the droplets towards the target. In another words, aerodynamic and electrical forces play an equally important role in the transport process of the droplets. Of course, the major purpose of the electrostatic support is to increase the transfer efficiency, i.e., the solid mass fraction of atomized paint that actually reaches the target may, which may exceed 90 % when using a large flat plate as target geometry.

The major operating conditions for the atomizer are given in table 1. At a bell diameter of 55 mm, the bell edge speed varies between 86 m/s at 30000 rev/min and 172 m/s at 60000 rev/min. For the present simulations, a silver metallic paint with a solid content of 18 % per mass was used. For a given paint the atomization process and, hence, the droplet size distribution depends on the liquid flow rate and the bell speed. As already reported in [1], the atomization process is characterized by the full ligament disintegration mode and the disintegration process is completed a few mm from the bell edge. Therefore, the initial droplet size distribution as very important inlet condition for the numerical simulations could be measured very close to the bell edge, using a Malvern Spraytec Fraunhofer type particle sizer. The initial droplet velocity vectors were derived from the bell speed.

Numerical Methods

The basic principles of the simulation of electrostatically supported rotary bell atomizers with corona charging have been reported before [2,3,4] and are not discussed in detail here. Basically, the corresponding modeling procedure can be divided into three different parts. The first aspect is concerned with the airflow field, the second is related to the modeling the electric field, and the last regards the motion of the droplet phase, where the interaction between the charged droplets with the airflow and the electric field is taken into account. The air flow field was modeled as fully 3-dimensional turbulent flow field, in most cases using the k-ε RNG turbulence model. Other turbulence models such as Re-Stress have been tested, however, the improvement in accuracy did not justify the significant additional computation time, which, as discussed below, is in the range of several days anyway.

The electric field including the space charge that is generated due to the imposed high voltage on the emitting electrode and the grounded work piece can be described by Poisson's equation and the conservation equation for the flow of the ions as follows:

$$\nabla^2 \Phi = -\frac{\rho}{\varepsilon} \qquad (1)$$

$$\mathbf{E} \cdot \nabla \rho = -\frac{\rho^2}{\varepsilon} \qquad (2)$$

The droplet phase was calculated using the well known Lagrangian approach with a stochastic tracking model. The coupling effect between two phase flows was taken into account, since the influence of the particulate phase on the airflow field could not be neglected especially at low shaping airflow rates. In general, the droplet trajectories were calculated by solving the equation of motion for the particles, extended by an additional term for the electric force $\mathbf{F}_E$,i.e.

$$\frac{d\mathbf{u}_\mathrm{p}}{dt} = f_D(\mathbf{u} - \mathbf{u}_\mathrm{p}) + \mathbf{F}_G + \mathbf{F}_E \ , \quad \frac{d\mathbf{x}}{dt} = \mathbf{u}_\mathrm{p} \quad (3)$$

Other forces, such as "virtual mass" and Saffman's lift force may be neglected. The electric force given in Eq. 3 is defined as follows

$$\mathbf{F}_E = q_p \mathbf{E} \qquad (4)$$

The droplet field charging, i.e. the charging due to the electrical field can be calculated according to *Pauthenier and Moreau-Hanot* [5]:

$$\frac{dq_\mathrm{p}}{dt} = \frac{q_s}{\tau}\left(1 - \frac{q_\mathrm{p}}{q_s}\right)^2 \qquad (5)$$

Here, the saturation charge q_s and the charging time constant τ are given by

$$q_s = \left[1 + 2\left(\frac{\varepsilon_\mathrm{r} - 1}{\varepsilon_\mathrm{r} + 2}\right)\right] 4\pi r_p^2 \varepsilon_0 E \quad (6)$$

$$\tau = \frac{4\varepsilon_0}{\rho\mu} \qquad (7)$$

Using Equation (5), the influence of the inhomogeneous electrical field (including space charge) and the different particle residence times in the corona discharge region on the particle charge may be taken into account.

Due to the complex flow field in the vicinity of the bell it is essential to define proper initial conditions for the airflow. In preliminary calculations it was found that the shaping air flow had to be calculated using the exact geometry, i.e., taking into account the individual nozzles in the shaping air ring behind the bell to obtain a correct velocity profile at the bell edge.

A local remeshing model available in FLUENT that is suitable for the relative boundary motions involving both translational and rotational movements had to be used. It was found that the so-called dynamic mesh model is most appropriate, since the real movement of the atomizer with respect to the car body is highly complicated. Figure 2 shows the grid for the simulation with a flat plate using the local remeshing model. The typical computational domain was 2 x 2 x 1.7 m³ with approximately 650 000 cells. In order to avoid difficulties and to keep the grid quality during the mesh movement, it is necessary to create a cylinder zone with interior boundary around the atomizer. Both the cylinder region and the atomizer are defined as moving zone. The initial position of the atomizer is located 300 mm away from the edge of the plate. During the movement the grid within the moving zone and the boundary layer mesh above the plate are not modified. An update of the grid topology in the dynamic zone is, however, performed after every time step. A detailed parameter setting in the remeshing model is given by in [6]. Despite all the modifications and adaptations mentioned above, the final dynamic grid was much coarser than the grid used in static calculations before. In the static case, a very fine prism layer was arranged in the region between atomizer and target, especially helpful for accurate calculations of the static electric field and the space charge.

So far, simple geometries of the grounded work piece, i.e., a flat plate and a 90° bended plate were used, both with a length of 1000 mm. The atomizer was moved horizontally above the plate along a straight line at constant velocity of 50 mm/s. The distance between atomizer and target surface was kept constant at 230 mm. This is a typical working distance in the practical application.

Results

For the flat plate case with the atomizer moving along the coordinate x, Figure 3 shows the resulting contour plots of the velocity field at different time steps. The corresponding operating conditions were 150 Nl/min shaping

air flow rate, 150 ml/min paint flow rate, bell speed 45 000 rev/min and a voltage of -45 000 V. At the positions where the atomizer is located outside of the flat plate, the velocity field is characterized by relatively narrow spray jets with velocity magnitudes extending 5-6 m/s even at the distance of the target. As soon as the atomizer moves above the plate, the boundary conditions for flow and electrostatic filed change significantly, resulting in a broader spray cone with reduced velocities. The paint film thickness distribution on the plate is plotted in Fig. 4, including also the profile of the local film thickness perpendicular to the direction of atomizer propagation at the center of the plate (x = 0). For the latter figure, the values are already converted into the dry film thickness, which may be easily compared to experimental results. Here, a very good agreement between measurement and simulation can be observed for both, the general shape and the width of the thickness profile as well as the local film thickness values. It should be noted that the uncertainty of the film thickness measurement probe is at least ± 1 µm. Of course, the difference in the transfer efficiency, i.e. the fraction of paint flow rate that is finally depositing on the target, is also quite small which can be derived from the areas under the film thickness profiles already.

A simulation using a slightly more complex target geometry, i.e., a bended plate, was also performed. The atomizer, operating in similar conditions as mentioned above, was moved horizontally with its axis exactly above the edge. Again, the working distance was 230 mm. The simulation results are plotted in Figure 5. The film thickness distribution along the edge is relatively stable. Of course, a higher film thickness can be observed on the horizontal part of the plate and close to the edge. On the vertical part of the plate there is also a significant part of the paint, which is basically the effect of the static electric field, however, the film thickness diminishes quickly with increasing distance from the edge. In agreement with the flat plate results, the simulations predict the experimental results almost perfectly.

Discussion

The simulations shown above were performed on a state-of-the-art PC type computer. For the given geometries and arrangements a CPU time of 144 hours was required applying a straight atomizer movement of 1.5 m. This is far too slow to solve any industrial problem, dealing with complicated 3-dimensional geometries like car bodies and very flexible atomizer paths. Moreover, it should be mentioned again that the dynamic grid had to be significantly coarser than the static grid used before, introducing visible differences especially in the calculation of the electric field and the space charge effect. In other words: The simulations have not yet reached a state of grid-independence.

In a sense, the results shown here have only intermediate character and demonstrate the principle feasibility of the chosen approach to include all physical effects and models into the FLUENT CFD-code. Of course, in the future parallel processing can be applied to improve the situation with respect to practically relevant cases and geometries. This requires a stable parallel solver for the discrete phase model including appropriate extensions with respect to electrical field and space charge, and all in combination with dynamic meshing models. However, it should be noted that simulation is a rather novel method in the painting industry, meaning that these companies and groups do not have easy access to high performance computers. Therefore, in most cases the quasi-dynamic spray painting simulation based on calculated static film thickness profiles might be a more appropriate approach, delivering film thicknesses on car body parts like bumpers or fenders in a few hours only.

Nomenclature

$\mathbf{E}$	electric field intensity	V/m
q_s	saturation charge	C
q_p	droplet charge	C
r_p	droplet radius	m
μ	ion mobility	m^2/Vs
ρ	space charge density	C/m^3
Φ	electrical potential	V
ε	electrical permittivity = $\varepsilon_r \varepsilon_0$	F/m
ε_r	relative electrical permittivity	-
ε_0	electrical permittivity of vacuum	F/m

References

1. Domnick, J., Thieme, M., Atomization and Sprays, 16: 857-874 (2006).
2. Ye, Q., Domnick, J., Scheibe, A., Pulli, K.: High Performance Computing in Science and Engineering'04, Springer-Verlag Berlin, Heidelberg, 261-275 (2004).
3. Domnick, J., Scheibe., A., Ye, Q., *Particle & Part. Syst. Char.*, 22:141-150 (2005).

4. Domnick, J., Scheibe., A., Ye, Q., *Particle & Part. Syst. Char.*, 23:408-416 (2006).
5. Pauthenier. M. M, Moreau-Hanot. M, J. Physique Radium 12 (1932), 590-613.
6. Wang, P., "Using moving mesh features to simulate dynamic electrostatic spray painting with a high-speed rotary bell and external charge", Master thesis, University of Stuttgart, 2005.

Table 1. Major operating conditions of the atomizer.

Bell diameter	55 mm (no serrations)
Bell material	Stainless steel
Rotary speed	40 000 - 60 000 1/min
Liquid flow rate	100 - 300 ml/min
High voltage	50-70 kV
Shaping air flow rate	80 - 300 l/min

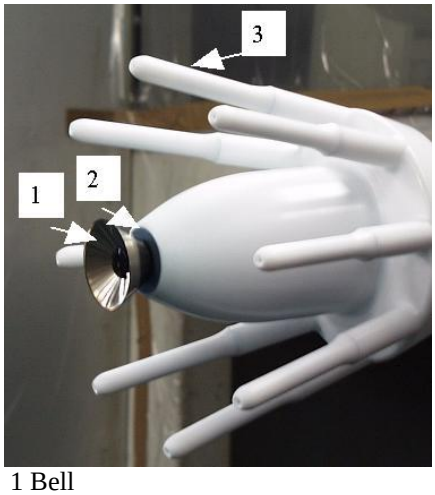

1 Bell
2 Shaping Air Ring
3 External Electrodes (External Charging)

Figure 1. Photograph of the external charging rotary bell atomizer

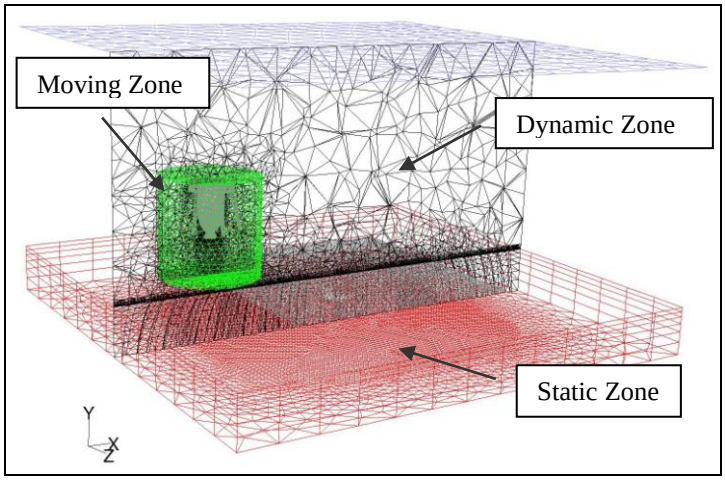

Figure 2. Adaptive numerical grid with the different zones

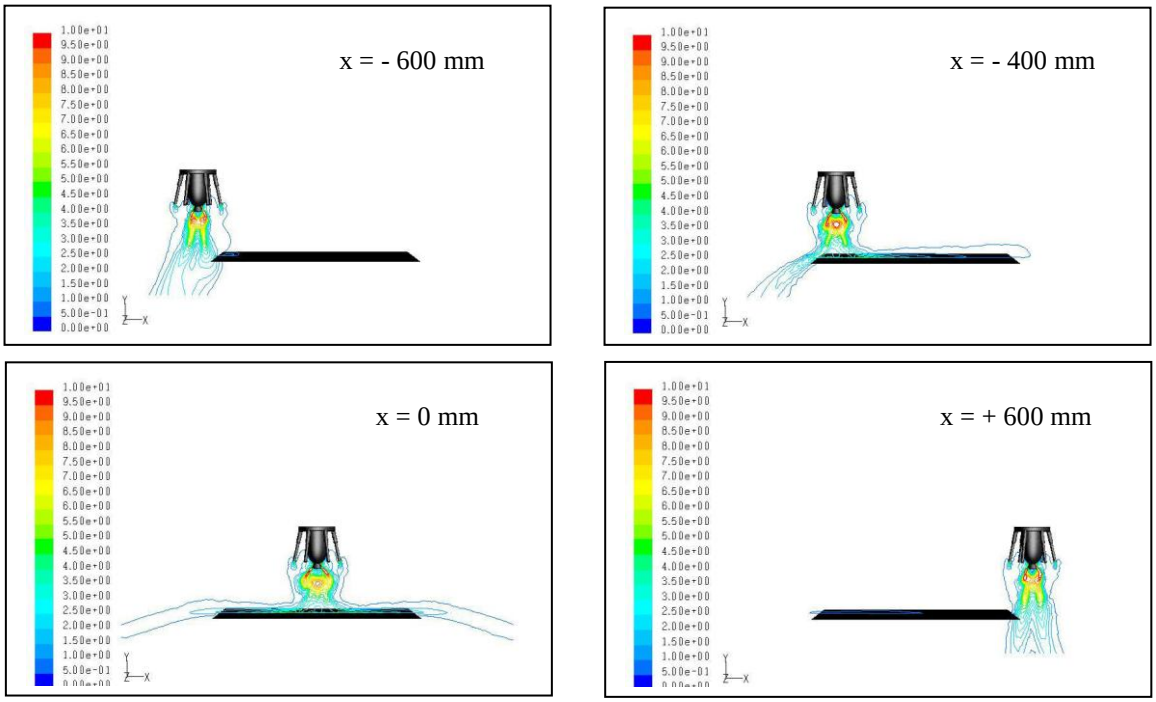

Figure 3: Flow field at different positions of the atomizer (Scale in m/s)

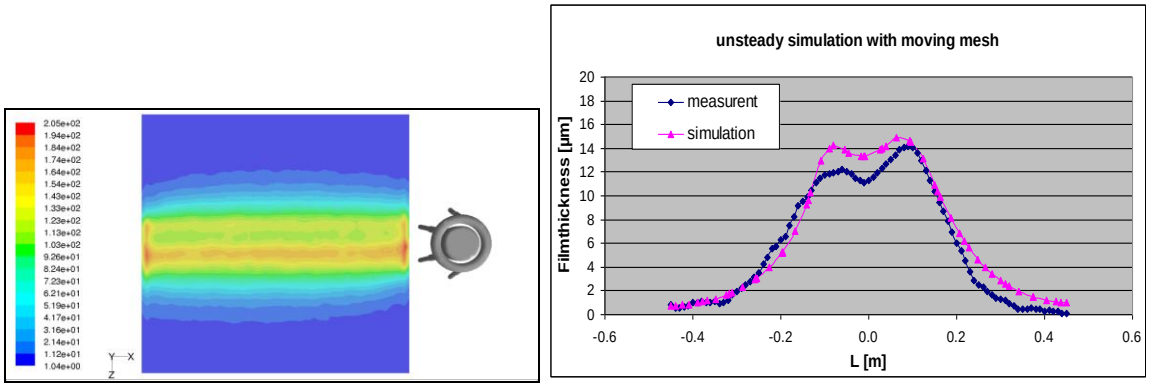

Figure 4: Contours of the wet film thickness (µm, left) and center line cross section (right) of dry film thickness

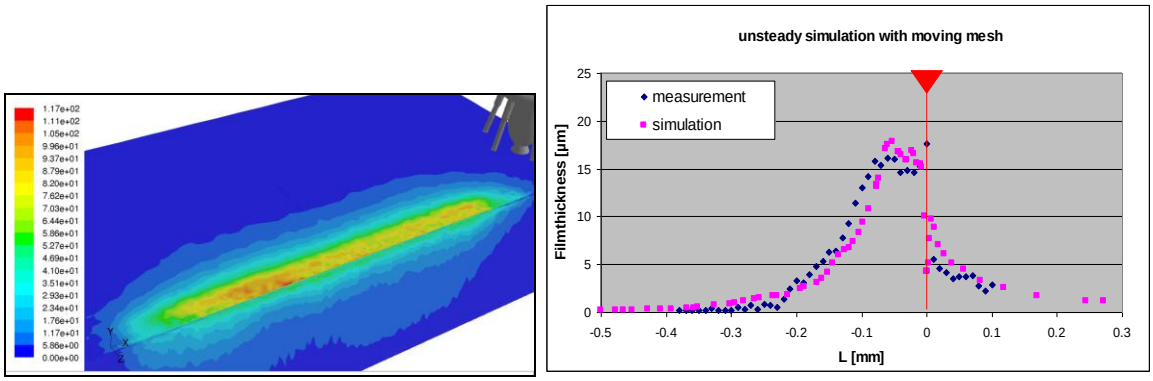

Figure 5: Wet film thickness (left) and center line cross section (right) of dry film thickness (bended plate)